

Four-hour thunderstorm nowcasting using deep diffusion models of satellite

Author Information

Kuai Dai, Xutao Li, Junying Fang, Yunming Ye, Demin Yu, Di Xian, Danyu Qin

Affiliations

School of Computer Science and Technology, Harbin Institute of Technology, Shenzhen, China

Kuai Dai, Xutao Li, Yunming Ye, Demin Yu

Institute of Tropical and Marine Meteorology, China Meteorological Administration, Guangzhou, China

Junying Fang

National Satellite Meteorological Center, China Meteorological Administration, Beijing, China

Di Xian, Danyu Qin

Contributions

Kuai Dai, Xutao Li, and Yunming Ye conceived and designed the work. Kuai Dai, Xutao Li, Yunming Ye, Demin Yu discussed details of the designed method and experimental results. Kuai Dai achieved the coding for the data process, model training, and results evaluation and completed manuscript writing. Junying Fang conducted investigation, visualization, and revision of the manuscript. Di Xian and Danyu Qin constructed the convection data and participated in data processing and case analysis. All the authors contributed edits.

Corresponding authors

Correspondence to: Xutao Li, lixutao@hit.edu.cn; Yunming Ye, yeyunming@hit.edu.cn

Abstract

Convection (thunderstorm) develops rapidly within hours and is highly destructive, posing a significant challenge for nowcasting and resulting in substantial losses to nature and society. After the emergence of artificial intelligence (AI)-based methods, convection nowcasting has experienced rapid advancements, with its performance surpassing that of physics-based numerical weather prediction and other conventional approaches. However, the lead time and coverage of it still leave much to be desired and hardly meet the needs of disaster emergency response. Here, we propose a deep diffusion model of satellite (DDMS) to establish an AI-based convection nowcasting system. On one hand, it employs diffusion processes to effectively simulate complicated spatiotemporal evolution patterns of convective clouds, significantly improving the forecast lead time. On the other hand, it utilizes geostationary satellite brightness temperature data, thereby achieving planetary-scale forecast coverage. During long-term tests and objective validation based on the FengYun-4A satellite, our system achieves, for the first time, effective convection nowcasting up to 4 hours, with broad coverage (about 20,000,000 km²), remarkable accuracy, and high resolution (15 minutes; 4 km). Its performance reaches a new height in convection nowcasting compared to the existing models. In terms of application, our system operates efficiently (forecasting 4 hours of convection in 8 minutes), and is highly transferable with the potential to collaborate with multiple satellites for global convection nowcasting. Furthermore, our results highlight the remarkable capabilities of diffusion models in convective clouds forecasting, as well as the significant value of geostationary satellite data when empowered by AI technologies.

Introduction

Severe convective weather often lead to sudden meteorological disasters like hailstorms, thunderstorms, strong winds, and tornadoes [1][2][3]. These events have significant adverse effects on various aspects of daily life and economic activities such as transportation, agriculture, energy production, and societal management [4][5][6]. As a conventional model for convective weather nowcasting and forecasting, the numerical weather prediction (NWP) solves the physical equations in the atmosphere to make predictions

[7]. While the NWP has advantages in large-scale weather forecast from several hours to several days ahead, it tends to produce poor results in local nowcasting from the present to several hours ahead [8][9], because the convection in mesoscale or small scale plays a crucial role. One alternative type of method is the advection-based approaches such as STEPS [10] or pySTEPS [11], which follow physical motion principles to extrapolate current states to the future. However, the advection-based approaches continue struggling to provide precise nowcasting outcomes due to two primary factors. On the one hand, the estimated advection tendency is unable to capture the intricateness of atmospheric motion and variation patterns, such as cloud formation and dissipation. On the other hand, these methods are limited in their ability to leverage extensive historical data for modeling nonlinear spatiotemporal dynamics, since they estimate the motion field based solely on the recent observations [12].

In recent years, artificial intelligence (AI) technologies [13][14][15] largely promote the forward of weather nowcasting [8][16]. With advanced neural network architectures [17][18][19][20][21], the AI-based nowcasting models learn spatiotemporal evolution patterns from historical meteorological data in an end-to-end optimization manner. Once trained, such models can efficiently make predictions with given observations. As a pioneer AI-based method for precipitation nowcasting, ConvLSTM [22] incorporates the convolution operation into LSTM [17] to model spatiotemporal patterns of radar sequences and delivers promising results compared with traditional approaches. To alleviate the blurry issue of nowcasting results produced by ConvLSTM, DGMR [8] introduces generative adversarial networks (GANs) [23][24][25][26] to improve the nowcasting results and achieves spatiotemporally consistent predictions with a lead time of 90 minutes. As a state-of-the-art precipitation nowcasting approach, NowcastNet [16] designs a special evolution network to learn physical knowledge to guide prediction and achieves 3-hour extreme precipitation prediction. Despite the progress delivered by such existing AI-based nowcasting approaches, they still fall short due to their limited lead time, spatial scale, and accuracy, especially in heavy rainfall closely related to convection.

As satellite remote sensing technologies advance rapidly, the latest generation of stationary meteorological satellites now offers extensive atmospheric monitoring capabilities, enabling them to

detect thunderstorm initiation earlier than radars [27][28][29][30][31][32]. For convective monitoring utilizing the infrared brightness temperature band, they can achieve a high spatiotemporal resolution quite close to that of ground-based radars. Furthermore, convection nowcasting with stationary satellite has gained widespread adoption in meteorological departments globally [33][34][35]. Compared to nowcasting convective activities based on ground-based radar data (whether from single stations or networked), a prominent advantage of nowcasting convection using brightness temperatures from geostationary satellites is the ability to monitor large areas at a planetary scale, including continuous 24-hour coverage of remote regions and oceans where radar installations do not exist. Recent studies [32] [36] introduce AI techniques to convection nowcasting with satellite data and achieve promising results. However, they provide accurate convection nowcasting results only in a short period (20 minutes – 2 hours). The essential reason is the lack of stable and reliable AI architectures designed to model the spatiotemporal evolution patterns of convective clouds, especially in the reasonable simulation of stochastic and uncertain motion patterns in the temporal evolution process of convective clouds. Inspired by the natural advantages of diffusion models in modeling stochastic processes [37], we argue that the stochastic motion tendency of convective clouds can be regarded as a physical diffusion process, which can be effectively modeled with forward and backward procedures of diffusion models [38][39].

Based on the insights above, we propose a deep diffusion model of satellite (DDMS) to establish a convective nowcasting system utilizing satellite brightness temperature data, and conduct long-term tests and objective validation based on the FengYun-4A satellite. This forecasting system achieves, for the first time, effective convection nowcasting up to 4 hours, and features key forecasting capabilities such as broad coverage (about 20,000,000 km²), high accuracy, and high spatiotemporal resolution (15 minutes; 4 km). Its performance reaches a new height in convection nowcasting compared to both the existing state-of-the-art AI models and the most advanced traditional models. Moreover, the forecasting system is highly transferable, with relevant methodologies and algorithms that can be easily transferred across different satellite platforms. It operates efficiently, forecasting 16 time points within 4 hours in just 8 minutes, possessing significant operational forecasting application advantages.

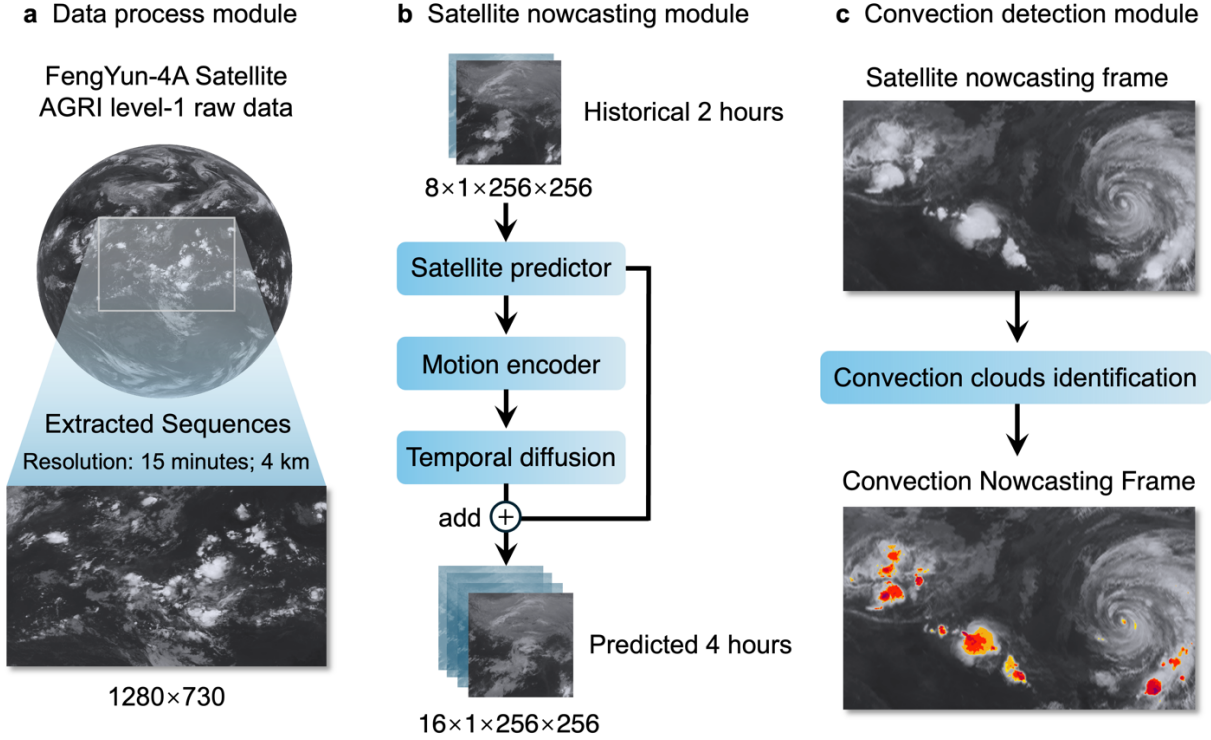


Figure 1 The overall framework of our high-resolution convection nowcasting system. Specifically, our system contains three modules, namely, a data process module, a satellite nowcasting module, and a convection detection module. **(a)** In the data process module, the collected FengYun-4A AGRI-L1-RGEC and DISK data are processed into regular satellite sequences through spatial cropping and temporal sampling operations. **(b)** In the satellite nowcasting module, the developed DDMS is trained to predict the next 4-hour satellite data based on the historical 2-hour satellite data. **(c)** In the convection detection module, a trained detection module is employed to identify the convective clouds in the predicted satellite sequences.

High-Resolution Convection Nowcasting System

We develop a high-resolution convection nowcasting system with deep learning techniques. Specifically, we formulate the convection nowcasting task as two stages, namely, satellite nowcasting and convection detection. For the satellite nowcasting, we propose the DDMS to model spatiotemporal patterns of convective clouds to predict the next 4-hour satellite sequences. For the convection detection, we adopt a combined manner of deep learning and expert knowledge to achieve the convective clouds recognition. In this article, we utilize FengYun-4A satellite data [40] from 2018 to 2021 year as training data and employ 2022 and 2023 data as the test data. The designed DDMS is trained on a GPU server

with eight RTX A6000 (48GB memory) and takes two million training batches to coverage (about 30 days).

As shown in **Figure 1**, the convection nowcasting system consists of a data process module, a satellite nowcasting module, and a convection detection module. First, in the data process module, collected FengYun-4A satellite images (AGRI-L1 RGECC and DISK data, 4km, 10.8 μ m-band) are first temporally sampled into sequences with a 15-minute interval, and then spatially cropped into 256×256 -size parts to reduce the GPU memory demand of satellite nowcasting module in the training phase. Second, the designed DDMS model is trained to predict the next 4-hour satellite sequences with historical 2-hour ones as input. Since our model is a fully convolutional network, once trained, it can be tested with arbitrary size sequences such as 1280×730 -size (about 20,000,000 km² coverage). Third, the convection detection module accounts for automatically recognizing the convective clouds in the predicted satellite sequences. To achieve this, we manually label a convective cloud dataset based on FengYun-4A with the guidance of experts in the National Satellite Meteorological Center and train an UNet to detect the convective clouds.

Through the three modules, we build a high-resolution convection nowcasting system. It significantly surpasses the state-of-the-art traditional nowcasting approach pySTEPS and the AI-based nowcasting method NowcastNet in terms of quantitative evaluation. Besides, in the severe convective weather events evaluation, our method accurately predicts the locations and intensity of convective clouds while the other baseline methods fail to do this.

Results

Evaluation Settings.

We validate the nowcasting ability of the proposed DDMS against the state-of-the-art traditional and AI-based prediction methods. For the traditional nowcasting method, we employ pySTEPS [11] as a baseline, an advection-based probabilistic nowcasting method, which has been widely used in meteorological centers worldwide [10] [41]. For the deep learning nowcasting methods, we select NowcastNet [16] as another baseline, which delivers state-of-the-art performance for 3-hour radar

nowcasting. In this work, we utilize FengYun-4A satellite 10.8 μ m-band observations in 2018-2021 years to train the models, and employ spring and summer samples (May to August) in 2022-2023 years to validate the nowcasting performance. In these months, the motions of convective clouds are fierce, and the clouds' growth and decay are common in the atmosphere, accompanied by abrupt meteorological disasters. Hence, we select the samples in spring and summer to verify the nowcasting ability of our model DDMS under such challenging scenarios.

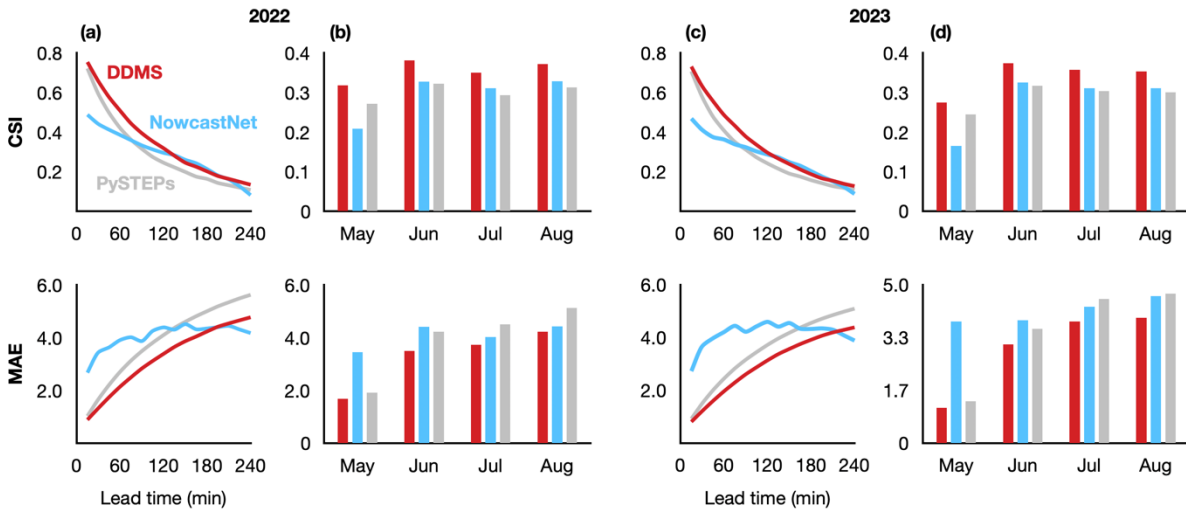


Figure 2 The quantitative convection nowcasting results of DDMS and the state-of-the-art baselines NowcastNet and pySTEPS. (a) The CSI and MAE curves w.r.t the time step, which are validated on FengYun-4A satellite samples in 2022 May to August. (b) The CSI and MAE scores of each month from May to August in 2022. (c) The CSI and MAE curves w.r.t the time step, which are validated on FengYun-4A satellite samples in 2023 May to August. (d) The CSI and MAE scores of each month from May to August in 2023.

Convection Nowcasting Results.

Quantitative Evaluation.

Figure 2 shows the quantitative convection nowcasting results of DDMS and state-of-the-art baseline methods NowcastNet and PySETPs. The critical success index (CSI) score is a key evaluation metric, which measures the nowcasting accuracy in terms of locations of convective clouds. The MAE represents the divergence between the predicted convection and the observation. Compared with the CSI score, the MAE score concentrates on reflecting the accuracy of predicted convection w.r.t the intensity. Overall,

the higher CSI score the better, while the lower MAE score the better. By analyzing the quantitative convection results, we have the following findings here.

First, in **Figure 2** (a) and (c), our approach DDMS significantly outperforms the traditional nowcasting baseline pySTEPS in both the CSI and MAE scores. Moreover, the advantage of our method becomes more obvious as the lead time goes by. The observations show the superiority of our model DDMS over pySTEPS in terms of predicting the location and intensity of convective clouds. As for the CSI score comparison, the state-of-the-art AI-based nowcasting baseline method NowcastNet merely delivers competitive results against the proposed DDMS during a short period (from 135 minutes to 195 minutes), while it performs much worse than DDMS during other periods. In addition, NowcastNet performs significantly worse than DDMS in terms of MAE score during the same short period. Similarly, NowcastNet significantly underperforms our DDMS on the MAE evaluation except for a short period (from 225 minutes to 240 minutes). However, during the same short period, NowcastNet performs the worst among the three approaches on the CSI evaluation. This indicates that The prediction ability of NowcastNet is insufficient, which cannot simultaneously balance the location and intensity of convective clouds. The observations show the significant superiority of our model DDMS for convection nowcasting results w.r.t different time steps.

Second, in **Figure 2** (b) and (d), we report convection nowcasting scores of DDMS and state-of-the-art baselines on May, Jun, July, and August months of 2022 and 2023 years. Obviously, our model DDMS delivers the best performance in all months in terms of CSI and MAE scores. The baseline methods pySTEPS and NowcastNet have their own advantages in different months. In terms of the CSI score, NowcastNet performs worse than pySTEPS in May months of 2022 and 2023, while it consistently surpasses pySTEPS in the other six months. In terms of the MAE score, NowcastNet performs worse than pySTEPS in May and June months of 2022 and 2023, while it has advantages in the other months. Specifically, in the 2022 year, the proposed DDMS outperforms pySTEPS (the second best) by 17.33% on CSI score in May, outperforms NowcastNet (the second best) by 16.38% on CSI score in June, by

12.89% on CSI score in July, by 13.35% on CSI score in August, respectively. In the 2023 year, the proposed DDMS outperforms pySTEPS (the second best) by 12.04% on CSI score in May, outperforms NowcastNet (the second best) by 14.99% on CSI score in June, by 14.93% on CSI score in July, by 13.54% on CSI score in August, respectively. As for the MAE score, DDMS outperforms pySTEPS (the second best) by 12.20% on MAE score in May, by 17.52% on MAE score in June, respectively, outperforms NowcastNet (the second best) by 7.48% on MAE score in July, by 4.61% on MAE score in August, respectively. In the 2023 year, the proposed DDMS outperforms pySTEPS (the second best) by 15.51% on MAE score in May, by 13.53% on MAE score in June, respectively, outperforms NowcastNet (the second best) by 10.84% on MAE score in July, by 14.76% on MAE score in August, respectively. The observations demonstrate that our DDMS can better model spatiotemporal patterns of convective clouds across different months while the state-of-the-art nowcasting baselines fail to do this.

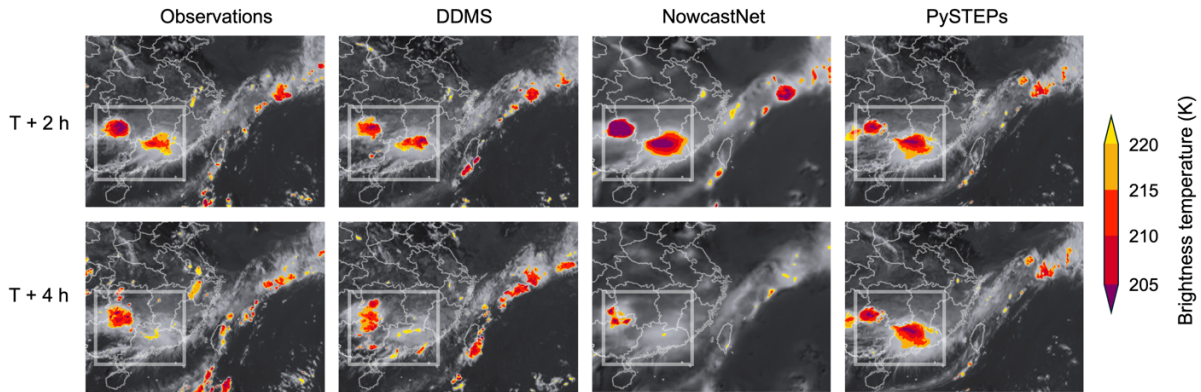


Figure 3 Case study of a severe convection event with extreme rainstorm starting on 16 June 2022, in south region of China. This convection event is also accompanied by floods warning of the Pearl River. The samples are cropped to highlight local details. The colored pixels denote the predicted convective clouds, and deeper color indicates higher intensity. The important part is marked with a white box. The state-of-the-art AI-based nowcasting baseline method NowcastNet significantly underestimates the motion tendency of convective clouds 4 hours later. The traditional baseline approach pySTEPS fails to model the growth and death of convective clouds and significantly overestimates the motion tendency of convective clouds. The two methods fail to deliver satisfactory 4-hour convection nowcasting, while our proposed DDMS produces much more accurate nowcasting results.

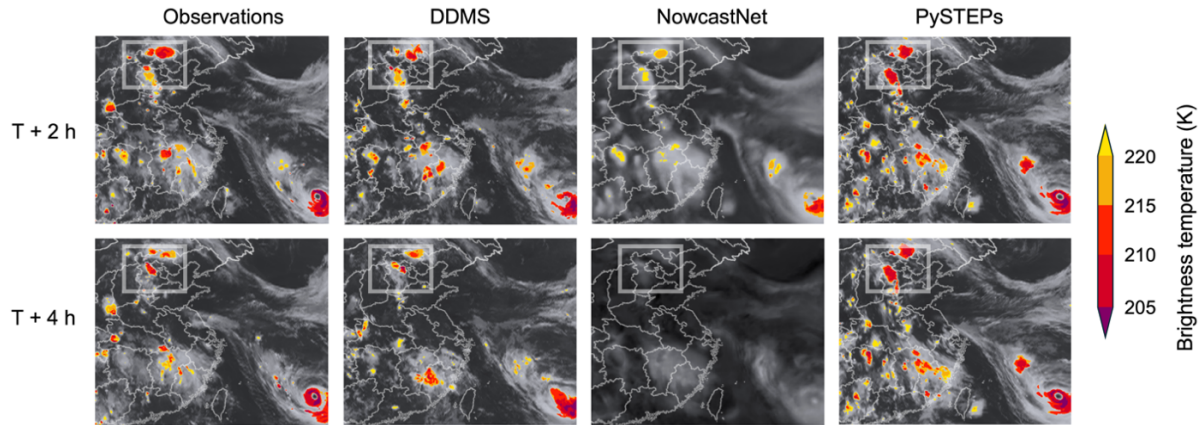


Figure 4 Case study of a severe convection event with extreme rainstorm starting on 29 July 2023, in Beijing-Tianjin-Hebei region of China. The samples are cropped to highlight local details. This convection event is affected by the typhoon Dusuirei (in the rightdown corner). The important part is marked with a white box. Again, our proposed DDMS delivers accurate nowcasting results while the state-of-the-art baselines fail to do this.

Severe Convection Events Nowcasting Comparison.

To visually compare the nowcasting ability of DDMS and state-of-the-art baselines, we show some nowcasting samples of severe convection events in **Figure 3** and **Figure 4**. We have following findings here by carefully comparing the nowcasting results. First, the advection-based baseline pySTEPS produces sharp yet inaccurate prediction results, which preserves sharp appearance details but fails to accurately predict the complicated motion tendency of clouds in the atmosphere. The 4-hour convection nowcasting results of pySTEPS are far away from the ground truth. This is because that the advection-based physical equations are hard to characterize the non-stationary motion patterns of clouds such as rotation, dissipation, and accumulation. Second, compared with pySTEPS, the state-of-the-art deep learning baseline NowcastNet makes more accurate predictions in the 2-hour nowcasting results, where the predicted convective clouds are more accurate in terms of locations, shape, and size. However, Nowcastnet delivers much more blurry nowcasting results. In addition, its prediction ability degrades dramatically, and can hardly deliver a useful prediction at 4 hours. Third, our method DDMS makes sharp predictions and delivers much more accurate 4-hour nowcasting results in terms of the location, size,

and intensity of convective clouds. The observations consistently show the advantages of our model DDMS for satellite nowcasting both in visual quality and prediction accuracy. The uncropped convection nowcasting samples are provided in the supplementary information file.

Discussion

In this article, we propose a deep diffusion model of satellite (DDMS) and build a high-resolution convection nowcasting system of satellite data. Our model is trained on 2018-2021 FengYun-4A satellite data and tested on 2022 and 2023 FenYun-4A satellite data. Compared with state-of-the-art nowcasting baseline approaches, the proposed method consistently delivers the best 4-hour nowcasting results in terms of quantitative evaluation and extreme convection events nowcasting comparison.

Though the developed DDMS can produce state-of-the-art 4-hour satellite nowcasting results, its training cost is one shortcoming due to the diffusion architecture. For this, it is necessary to explore more efficient diffusion models [42][43]. Despite the larger training cost of the proposed DDMS compared with the AI-based method NowcastNet, our developed high-resolution convection nowcasting system can produce 4-hour convection nowcasting with broad coverage (about 20,000,000 km²), in 8 minutes, which easily satisfies the nowcasting requirements in practical scenarios.

Looking into the future, convection nowcasting can be further improved from many diverse aspects. In terms of methodology, more efficient AI techniques can be explored to deliver more accurate and higher spatio-temporal resolution convection nowcasting. Besides, from the perspective of data, fusing multi-source such as satellite and radar data can promote the accuracy and interpretability of AI-based methods for convection nowcasting. At last, explicitly incorporating the conventional physical knowledge as constraint for AI-based methods is a promising direction. We hope this work can inspire more researchers to investigate convection nowcasting with meteorological satellite data.

Methods

Here we introduce the details of the data process module, satellite nowcasting module, and convection detection module in the high-resolution convection nowcasting systems, as well as the evaluation metrics and training settings.

Data Process Module.

In this article, we collect FengYun-4A meteorological satellite AGRI-L1 data, from 2018 to 2023 year. Data in 2018-2021 years are utilized for training satellite nowcasting module while the remainder part is for convection nowcasting evaluation. With a multichannel visible infrared scanning imager, FengYun-4A can produce 14-waveband satellite images, where different wavebands aim at capturing different meteorological elements such as water vapor and temperature. To achieve convection nowcasting, we select the 12-th channel (10.8 μ m-band, long-wave infrared) images with 4km spatial resolution, which is suitable for observing the convective clouds in the atmosphere. The FengYun-4A satellite scans the China area (REGC) and the entire observation area (DISK) with an interval of 4-6 minutes and 15 minutes, respectively. First, we extract 24-frame sequences with an interval of 15 minutes, where each frame is 1280 \times 730-size. Second, to save the training memory demand, we crop 256 \times 256-size parts of each frame. In this manner, we obtain 441,895 sequences for training the satellite nowcasting module and 4355 sequences for validation, respectively.

Satellite Nowcasting Module.

As shown in **Figure 5**, the module consists of three parts, namely, a satellite predictor P , a motion encoder M , and a temporal diffusion part D . First, the satellite predictor accounts for producing the predicted satellite sequence $\hat{Y} = \{\hat{X}_{l+1}, \hat{X}_{l+2}, \dots, \hat{X}_{l+k}\} \in \mathbb{R}^{k \times m \times n}$, with given the past frames $X = \{X_1, X_2, \dots, X_l\} \in \mathbb{R}^{l \times m \times n}$. m and n denote the width and length of each satellite image, respectively. Second, the temporal diffusion part is specially designed to model the temporal evolution dynamics of divergence between the predicted sequence \hat{Y} and ground truth sequence $Y = \{X_{l+1}, X_{l+2}, \dots, X_{l+k}\}$. Third,

the motion encoder is designed to capture the long-term motion tendency of the predicted sequence \hat{Y} , to guide the denoising process of the temporal diffusion part. By combining the predicted sequence by satellite predictor P and the reconstructed difference sequence by temporal diffusion D , we obtain the final prediction sequence $\hat{Y}_{final} = P(x) + D(Y - \hat{Y})$. Next, we introduce details of the three parts and the training loss of the satellite nowcasting module.

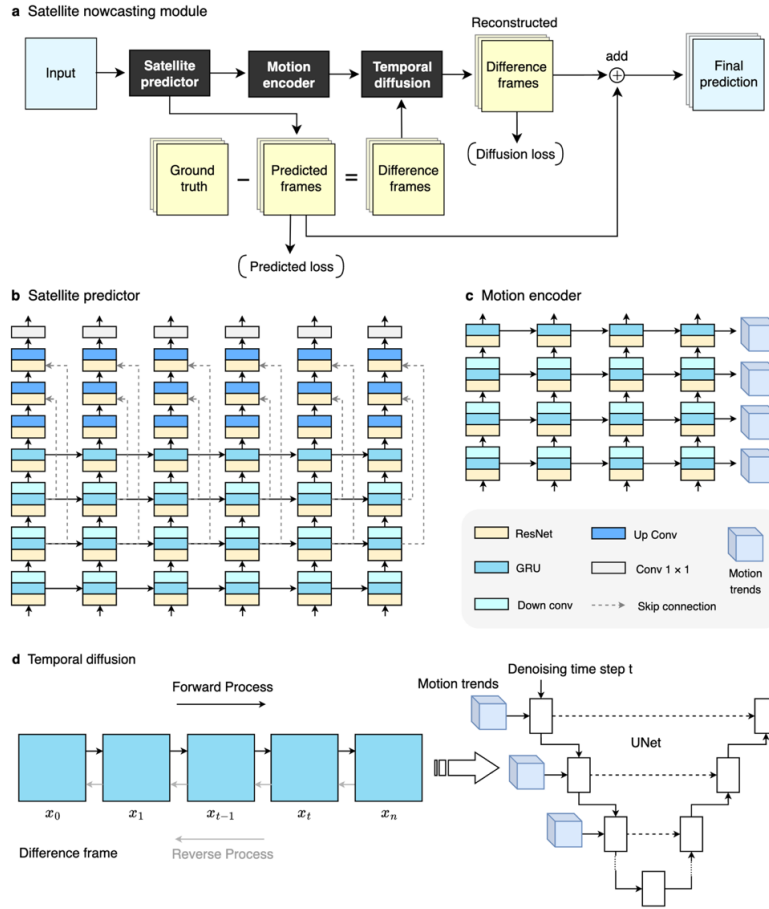


Figure 5 The pipelines of the satellite nowcasting module. (a) The overall layout of the satellite nowcasting module, which contains a satellite predictor, a motion encoder, and a temporal diffusion part. The satellite predictor accounts for producing the predicted sequence with given historical frames. With the guidance of the motion encoder, the temporal diffusion part aims to model temporal evolution dynamics of difference sequences between the prediction and ground truth. The final prediction is obtained by combining the predicted sequence and the reconstructed difference sequence. (b) The architecture details of the satellite predictor, which contains multiscale GRU units. (c) The architecture details of the motion encoder, which is an encoder part of the satellite predictor and has independent parameters. (d) The workflow of the temporal diffusion part for i -th difference satellite frame. The conditional Unet is employed to predict a noise in the reverse process.

Satellite Predictor. Overall, the satellite predictor follows a classic RNN architecture ConvGRU [14], which is a simple yet effective spatiotemporal prediction baseline. Specifically, it contains an encoder part and a decoder part. In the encoder, three ResNet-GRU-Conv block layers and one ResNet-GRU block layer are utilized to encode multi-level spatiotemporal dynamics of satellite sequences. In the decoder, three ResNet-DeConv block layers and one convolutional layer with a kernel size of 1 are employed to produce predicted frames by decoding the multi-level spatiotemporal features. Notably, in each time step, different level hidden states generated by the GRU units in the encoder are passed to the decoder with a skip connection manner, which can better preserve spatial details.

Motion Encoder. The motion encoder adopts the previous four layers of a satellite predictor to encode the predicted sequence to obtain the long-term motion patterns, which are utilized to guide the denoising process of the temporal diffusion part. In particular, the motion encoder does not share parameters with the satellite predictor.

Temporal Diffusion. With the guidance of the motion encoder, the temporal diffusion part is proposed to model the temporal evolution of the difference satellite sequence. To train the diffusion network, we adopt a training paradigm provided by DDPM [38], which treats the diffusion process as a first-order Markov-chain procedure. Specifically, in the forward process, Gaussian noise is gradually added to destroy the original data x_0 , then we obtain T different states $\{x_1, x_2, \dots, x_T\}$, which is formally defined as follows:

$$q(x_{1:T} | x_0) = \prod_{t=1}^T q(x_t | x_{t-1}), \quad (1)$$

$$q(x_t | x_{t-1}) = \mathcal{N}(x_t | \sqrt{\alpha_t}x_{t-1}, (1 - \alpha_t)\mathbf{I}). \quad (2)$$

$1 - \alpha_t$ is the predefined covariance hyperparameter at the t -th time step. $\alpha_t \in (0,1), t \in \{1,2, \dots, T\}$, and $\alpha_1 > \alpha_2 > \dots > \alpha_T$. Through formulae (1) and (2), t -th state x_t can be obtained in one step as follows:

$$q(x_t | x_0) = \int q(x_{1:t} | x_0) dx_{1:(t-1)} = \mathcal{N}(x_t | \sqrt{\bar{\alpha}_t} x_0, (1 - \bar{\alpha}_t) \mathbf{I}), \quad (3)$$

where $\bar{\alpha}_t = \alpha_1 \alpha_2 \dots \alpha_t$. When $t \rightarrow \infty$, then $\bar{\alpha}_t \rightarrow 0$, and we can get that $x_t \rightarrow \mathcal{N}(0, \mathbf{I})$.

In the reverse process, we aim to recover the original data x_0 from the Gaussian noise x_T . Formally, the denoising process is defined as follows:

$$p(x_0) = \int p(x_{0:T}) dx_{1:T}, \quad (4)$$

$$p(x_{0:T}) = p(x_T) \prod_{t=1}^T p(x_{t-1} | x_t), \quad (5)$$

$$p(x_{t-1} | x_t) = \mathcal{N}(x_{t-1} | \mu(x_t, t), \sigma_t \mathbf{I}). \quad (6)$$

The $p(x_T) = \mathcal{N}(0, \mathbf{I})$ is known, and the σ_t is fixed and computed by $\bar{\alpha}_t$. The mean value $\mu(x_t, t)$ needs to be learned and depends on Gaussian noise. For this, DDPM adopts a UNet model f_θ to predict the noise ϵ . In this work, we employ the global motion patterns $M(\hat{Y})$ of the predicted sequence as a condition to help the UNet to predict the noise. Hence, the training loss function of the denoising process is as follows:

$$L(\theta) = \mathbb{E}_{\mathbf{x}_0, t, \epsilon} \|\epsilon - f_\theta(\mathbf{x}_t, t, M(\hat{Y}))\|^2, \quad (7)$$

$$x_t = \sqrt{\bar{\alpha}_t} x_0 + \sqrt{1 - \bar{\alpha}_t} \epsilon. \quad (8)$$

Training Loss. We employ a predicted loss, namely, mean absolute error loss, to train the satellite predictor. We use a diffusion loss to train the temporal diffusion part. By combining the two loss terms, we obtain the training loss of the satellite nowcasting module as follows:

$$L(\hat{Y}, Y) = \sum_{i=1}^k (|Y_i - \hat{Y}_i| + \lambda * Diff(Y_i - \hat{Y}_i)). \quad (9)$$

The coefficient λ is utilized to balance the two loss terms. $Diff(.)$ is implemented by optimizing formulae (7) and (8), where the initial state $x_0 = Y_i - \hat{Y}_i$.

Convection Detection Module.

Traditional convection detection on satellite images usually relies on a specific threshold value to judge convective clouds, in which the threshold value is obtained according to meteorologists's experiential judgment. As for the 10.8 μ m-band FengYun-4A data, the grids are regarded as convective clouds, whose brightness temperature of each grid is lower than 210K (provided by the National Satellite Meteorological Center). The threshold detection approach is simple but not very robust, and its accuracy is also a main concern. To automatically detect the convective clouds in the predicted satellite sequence, our team and experts in the National Satellite Meteorological Center manually label a convection dataset. Specifically, we label the convective clouds by combining four principles, namely, the basic characteristics of convective clouds summarized by experts, satellite images in visible channels, the brightness temperature of satellite data, and corresponding radar maps. Then we utilize the convection dataset to train a detection model (2D-UNet [44]). Finally, the convection nowcasting results are obtained by segmenting each frame of the predicted satellite sequence produced by the satellite nowcasting module with the pretrained detection model.

Evaluation Metrics.

For quantitative evaluation, we utilize two commonly used metrics in weather nowcasting including critical success index (CSI) and mean absolute error (MAE) to evaluate the convection nowcasting results.

Both the CSI and MAE scores measure nowcasting accuracy, the CSI emphasizes location while MAE concentrates on intensity. The metrics are formally defined as follows:

$$CSI = \frac{TP}{TP + FN + FP}, \quad (10)$$

$$MAE = |\hat{Y}_{final} \odot \hat{C} - Y \odot C|. \quad (11)$$

With the convection detection module, the predicted satellite sequences \hat{Y}_{final} are binarized to the convection sequences \hat{C} . Then we can obtain the true positives (TP, prediction = 1, target = 1), false positives (FP, prediction = 1, target = 0), and false negatives (FN, prediction = 0, target = 1), to calculate the CSI score. The Y and C represent the ground-truth satellite sequences and corresponding detection results, respectively. The \odot denotes the Hadamard product, and the MAE is obtained by computing the error between the predicted convection results $\hat{Y}_{final} \odot \hat{C}$ and convection observations $Y \odot C$.

Implementation Details.

Our model DDMS is trained on a GPU server with a CPU of Intel(R) Xeon(R) Gold 6130 CPU @ 2.10GHz, 256G memory, and 8 RTX A6000 cards (48G memory). We utilize the Adam optimizer [45] to train the model, and use the exponential moving average (EMA) strategy [46] with a decay weight of 0.99 to update the parameters. The batch size and learning rate are set to 8 and 5e-5, respectively. The weight λ in the combined training loss is 10. The dimensions of hidden states in the four-layer GRU are set to 64, 128, 192, and 256, respectively. As for the diffusion part, the forwarding step is set to 1000, while the denoising step is set to 200 with a DDIM [39] sampling manner. The details and analysis of our model are shown in the supplementary material.

Data Availability

The FengYun-4A AGRI-4km-L1 satellite data (about 18T) can be free downloaded from the website [<http://data.nsmc.org.cn/portalsite/default.aspx>]. The satellite data comprises two types: DISK and REGC. DISK data covers the entire disk region, while REGC data specifically focuses on the China area. We combine these two types of data and extract sequences of 24 frames at 15-minute intervals. In addition, the test satellite data and corresponding labeled convection data will be provided soon.

Code Availability

In this work, we utilize pytorch [<https://pytorch.org/>], a widely used deep learning framework, to train our model. We use Python [<https://www.python.org/>] to complete the data process and results evaluation. In particular, we use the h5py to load the FengYun-4A HDF files and employ opencv-python to read and save the processed satellite images. The quantitative metrics such as CSI and MAE are calculated on the Python library Numpy. Besides, we utilize the pySTEPS [<https://pysteps.github.io/>] and NowcastNet [<https://codeocean.com/capsule/3935105/tree/v1>] as baselines to achieve convection nowcasting. The source codes of DDMS and its pretrained weight will be provided soon.

References

1. Dotzek, N., Groenemeijer, P., Feuerstein, B., & Holzer, A. M. Overview of ESSL's severe convective storms research using the European Severe Weather Database ESWD. *Atmospheric research*, 93 (1-3), 575-586 (2009).
2. Melhauser, C., & Zhang, F. Practical and intrinsic predictability of severe and convective weather at the mesoscales. *Journal of the Atmospheric Sciences*, 69 (11), 3350-3371 (2012).
3. Tippett, M. K., Allen, J. T., Gensini, V. A., & Brooks, H. E. Climate and hazardous convective weather. *Current Climate Change Reports*, 1, 60-73 (2015).
4. Castle, J., Hendry, D., & Kitov, O. *Forecasting and nowcasting macroeconomic variables: A methodological overview*. (Press, Eurostat, 2017).
5. Wilson, J. W., Feng, Y., Chen, M., & Roberts, R. D. Nowcasting challenges during the Beijing Olympics: Successes, failures, and implications for future nowcasting systems. *Weather and Forecasting*, 25 (6), 1691-1714 (2010).
6. Han, L., Sun, J., Zhang, W., Xiu, Y., Feng, H., & Lin, Y. A machine learning nowcasting method based on real-time reanalysis data. *Journal of Geophysical Research: Atmospheres*, 122 (7), 4038-4051 (2017).

7. Toth, Z., & Kalnay, E. Ensemble forecasting at NCEP and the breeding method. *Monthly Weather Review*, 125 (12), 3297-3319 (1997).
8. Ravuri, S., Lenc, K., Willson, M., Kangin, D., Lam, R., Mirowski, P., ... & Mohamed, S. Skilful precipitation nowcasting using deep generative models of radar. *Nature*, 597 (7878), 672-677 (2021).
9. Pierce, C., Seed, A., Ballard, S., Simonin, D. & Li, Z. Doppler radar observations: Weather radar, wind profiler, ionospheric radar, and other advanced applications. (eds Bech, J. & Chau, J. L.) 97–142 (IntechOpen, 2012).
10. Bowler, N. E., Pierce, C. E., & Seed, A. W. STEPS: A probabilistic precipitation forecasting scheme which merges an extrapolation nowcast with downscaled NWP. *Quarterly Journal of the Royal Meteorological Society*, 132 (620), 2127-2155. (2006).
11. Pulkkinen, S., Nerini, D., Pérez Hortal, A. A., Velasco-Forero, C., Seed, A., Germann, U., & Foresti, L. Pysteps: An open-source Python library for probabilistic precipitation nowcasting (v1. 0). *Geoscientific Model Development*, 12 (10), 4185-4219 (2019).
12. Dai, K., Li, X., Ye, Y., Feng, S., Qin, D., & Ye, R. MSTCGAN: Multiscale time conditional generative adversarial network for long-term satellite image sequence prediction. *IEEE Transactions on Geoscience and Remote Sensing*, 60, 1-16. (2022).
13. Shi, X., Chen, Z., Wang, H., Yeung, D. Y., Wong, W. K., & Woo, W. C. Convolutional LSTM network: A machine learning approach for precipitation nowcasting. *Proceedings of the Advances in neural information processing systems*, 28 (2015).
14. Ballas, N., Yao, L., Pal, C., & Courville, A. Delving deeper into convolutional networks for learning video representations. *Proceedings of the International Conference on Learning Representations* (2015).

15. Wang, Y., Wu, H., Zhang, J., Gao, Z., Wang, J., Philip, S. Y., & Long, M. Predrnn: A recurrent neural network for spatiotemporal predictive learning. *IEEE Transactions on Pattern Analysis and Machine Intelligence*, 45 (2), 2208-2225 (2022).
16. Zhang, Y., Long, M., Chen, K., Xing, L., Jin, R., Jordan, M. I., & Wang, J. Skilful nowcasting of extreme precipitation with NowcastNet. *Nature*, 619 (7970), 526-532 (2023).
17. Hochreiter, S., & Schmidhuber, J. Long short-term memory. *Neural computation*, 9 (8), 1735-1780 (1997).
18. Chung, J., Gulcehre, C., Cho, K., & Bengio, Y. Empirical evaluation of gated recurrent neural networks on sequence modeling. *Proceedings of the Advances in neural information processing systems workshop* (2014).
19. Krizhevsky, A., Sutskever, I., & Hinton, G. E. Imagenet classification with deep convolutional neural networks. *Proceedings of the Advances in neural information processing systems*, 25 (2012).
20. Vaswani, A., Shazeer, N., Parmar, N., Uszkoreit, J., Jones, L., Gomez, A. N., Kaiser, Ł. & Polosukhin, I. Attention is all you need. *Proceedings of the Advances in neural information processing systems*, 30 (2017).
21. Bi, K., Xie, L., Zhang, H., Chen, X., Gu, X., & Tian, Q. Accurate medium-range global weather forecasting with 3D neural networks. *Nature*, 619(7970), 533-538 (2023).
22. Shi, X., Chen, Z., Wang, H., Yeung, D. Y., Wong, W. K., & Woo, W. C. Convolutional LSTM network: A machine learning approach for precipitation nowcasting. *Proceedings of the Advances in neural information processing systems*, 28 (2015).
23. Goodfellow, I., Pouget-Abadie, J., Mirza, M., Xu, B., Warde-Farley, D., Ozair, S., Courville, A. & Bengio, Y. Generative adversarial nets. *Proceedings of the Advances in neural information processing systems*, 27 (2014).

24. Radford, A., Metz, L., & Chintala, S. Unsupervised representation learning with deep convolutional generative adversarial networks. Proceedings of the International Conference on Learning Representations (2015).
25. Arjovsky, M., Chintala, S., & Bottou, L. Wasserstein generative adversarial networks. Proceedings of the International Conference on Machine Learning, 214-223 (2017).
26. Miyato, T., Kataoka, T., Koyama, M., & Yoshida, Y. Spectral Normalization for Generative Adversarial Networks. Proceedings of the International Conference on Learning Representations (2018).
27. Sieglaff, J. M., Counce, L. M., Feltz, W. F., Bedka, K. M., Pavolonis, M. J., & Heidinger, A. K. Nowcasting convective storm initiation using satellite-based box-averaged cloud-top cooling and cloud-type trends. Journal of applied meteorology and climatology, 50 (1), 110-126 (2011).
28. Kober, K., & Tafferner, A. Tracking and nowcasting of convective cells using remote sensing data from radar and satellite. Meteorologische Zeitschrift, 1, 75-84 (2009).
29. Bedka, K., Brunner, J., Dworak, R., Feltz, W., Otkin, J., & Greenwald, T. Objective satellite-based detection of overshooting tops using infrared window channel brightness temperature gradients. Journal of applied meteorology and climatology, 49 (2), 181-202 (2010).
30. Ai, Y., Li, J., Shi, W., Schmit, T. J., Cao, C., & Li, W. Deep convective cloud characterizations from both broadband imager and hyperspectral infrared sounder measurements. Journal of Geophysical Research: Atmospheres, 122 (3), 1700-1712 (2017).
31. Takahashi, H., & Luo, Z. J. Characterizing tropical overshooting deep convection from joint analysis of CloudSat and geostationary satellite observations. Journal of Geophysical Research: Atmospheres, 119 (1), 112-121 (2014).

32. Lagerquist, R., Stewart, J. Q., Ebert-Uphoff, I., & Kumler, C. Using deep learning to nowcast the spatial coverage of convection from Himawari-8 satellite data. *Monthly Weather Review*, 149(12), 3897-3921 (2021).
33. Mecikalski, J. R., Rosenfeld, D., & Manzato, A. Evaluation of geostationary satellite observations and the development of a 1–2 h prediction model for future storm intensity. *Journal of Geophysical Research: Atmospheres*, 121(11), 6374-6392 (2016).
34. Walker, J. R., MacKenzie Jr, W. M., Mecikalski, J. R., & Jewett, C. P. An enhanced geostationary satellite-based convective initiation algorithm for 0–2-h nowcasting with object tracking. *Journal of Applied Meteorology and Climatology*, 51(11), 1931-1949 (2012).
35. Mecikalski, J. R., & Bedka, K. M. Forecasting convective initiation by monitoring the evolution of moving cumulus in daytime GOES imagery. *Monthly Weather Review*, 134(1), 49-78 (2006).
36. Lee, S., Han, H., Im, J., Jang, E., & Lee, M. I. Detection of deterministic and probabilistic convection initiation using Himawari-8 Advanced Himawari Imager data. *Atmospheric Measurement Techniques*, 10(5), 1859-1874 (2017).
37. Sohl-Dickstein, J., Weiss, E., Maheswaranathan, N., & Ganguli, S. Deep unsupervised learning using nonequilibrium thermodynamics. *Proceedings of the International Conference on Machine Learning* 2256-2265 (2015).
38. Ho, J., Jain, A., & Abbeel, P. Denoising diffusion probabilistic models. *Proceedings of the Advances in Neural Information Processing Systems*, 33, 6840-6851 (2020).
39. Song, J., Meng, C., & Ermon, S. Denoising diffusion implicit models. *Proceedings of the International Conference on Learning Representations* (2020).
40. Xian, D., Zhang, P., Gao, L., Sun, R., Zhang, H., & Jia, X. Fengyun meteorological satellite products for earth system science applications. *Advances in Atmospheric Sciences*, 38(8), 1267-1284 (2021).

41. Imhoff, R. O., Brauer, C. C., Overeem, A., Weerts, A. H., & Uijlenhoet, R. Spatial and temporal evaluation of radar rainfall nowcasting techniques on 1,533 events. *Water Resources Research*, 56 (8), e2019WR026723 (2020).
42. Rombach, R., Blattmann, A., Lorenz, D., Esser, P., & Ommer, B. High-resolution image synthesis with latent diffusion models. *Proceedings of the IEEE/CVF conference on computer vision and pattern recognition*, 10684-10695 (2022).
43. Blattmann, A., Rombach, R., Ling, H., Dockhorn, T., Kim, S. W., Fidler, S., & Kreis, K. Align your latents: High-resolution video synthesis with latent diffusion models. *Proceedings of the IEEE/CVF Conference on Computer Vision and Pattern Recognition*, 22563-22575 (2023).
44. Ronneberger, O., Fischer, P., & Brox, T. U-net: Convolutional networks for biomedical image segmentation. *Proceedings of the Medical Image Computing and Computer-Assisted Intervention, Part III 18*, 234-241 (2015).
45. Kingma, D. P., & Ba, J. Adam: A method for stochastic optimization. *Proceedings of the International Conference on Learning Representations* (2015).
46. Tarvainen, A., & Valpola, H. Mean teachers are better role models: Weight-averaged consistency targets improve semi-supervised deep learning results. *Proceedings of the Advances in Neural Information Processing Systems*, 30, 1195-1204 (2017).

Acknowledgements

This work was supported by NSFC under Grants 62376072, 62272130, and Shenzhen Science and Technology Program under Grant JCYJ20200109113014456 and Grant KCXFZ20211020163403005, Guangdong Basic and Applied Basic Research Foundation (2023A1515110811, J.F.), and FengYun Application Pioneering Project under Grant FY-APP-ZX-2022.0220.

Ethics declarations

Competing interests

The authors declare no competing interests.